Gas-Phase Hydrogenation of *o*-Xylene over Pt/Knitted Silica-Fiber Catalysts

A. Kalantar Neyestanaki,*,† P. Mäki-Arvela,† H. Backman,† H. Karhu,†,‡ T. Salmi,† J. Väyrynen,‡ and D. Yu. Murzin*,†

Laboratory of Industrial Chemistry, Process Chemistry Group, Åbo Akademi, Biskopsgatan 8, FIN-20500 Åbo/Turku, Finland, Department of Physics, University of Turku, Vesilinnantie 5, FIN-20014 Åbo/Turku, Finland

A knitted silica fiber was prepared and employed as a support material for platinum catalysts. Different knitted silica-fiber supported platinum catalysts were prepared using several platinum precursors. The catalysts were characterized by N_2 physisorption, H_2 adsorption, $NH_3/H_2/o$-xylene temperature-programmed desorption, scanning electron microscopy−energy-dispersive X-ray analysis, and X-ray photoelectron microscopy. Catalyst activity was investigated in the gas-phase hydrogenation of *o*-xylene at 360−460 K with *o*-xylene and hydrogen partial pressures of 0.06 and 0.36−0.73 bar. High *o*-xylene conversions (up to 99%) to *cis*- and *trans*-1,2-dimethylcyclohexane were achieved. The specific surface area and pore volume of the support and the platinum precursor affected the catalyst performance. A catalyst prepared from platinum nitrate with a metal loading of 5 wt % exhibited the highest hydrogenation activity. A maximum in hydrogenation activity vs temperature was observed, which was caused by decreased surface *o*-xylene coverage with a temperature increase. Residual surface chlorine was found to affect both the catalyst activity and the product stereoselectivity. The selectivity toward the formation of *trans*-1,2-dimethylcyclohexane is increased at higher operation temperatures.

Introduction

Catalytic hydrogenation of aromatic hydrocarbons is applied in the oil-refining industry to suppress the amount of undesired aromatics in solvents and diesel fuels. The rate of aromatic hydrogenation is strongly affected by steric factors because the hydrogenation rate decreases by substitution of alkyl groups to the aromatic ring and an increase of the length of the substituent.[1−7] Benzene and, to a lesser extent, toluene have been frequently used as model reactants for aromatic hydrogenation. The kinetics of gas-phase hydrogenation of xylenes has been investigated over supported Pd,[7−10] Ru,[10,11] Ni,[12−15] and Pt[16−19] catalysts. The relative position of the substituents has a significant effect on the reaction rate, which decreases in the order *p*-xylene > *m*-xylene > *o*-xylene. Similar to benzene and toluene hydrogenation, a reversible temperature dependency of the activity maximum in xylene hydrogenation is observed.[12−15,17] The turnover frequencies in hydrogenation of xylenes are reported to increase by support acidity,[7] and this was explained by the adsorption of aromatics on the carrier. The nature of the catalyst as well as the operation conditions has a strong effect on the product stereoselectivity. The selectivity to the formation of thermodynamically favored *trans*-1,2-dimethylcyclohexane is reported to be enhanced by the temperature, metal dispersion, and acidity of the support.[8−15,18,19] Recently, the interest for structured catalysts such as monoliths, catalyst packing, and fibers has considerably increased. The major benefits of fibrous materials are their low-pressure drop induction and short diffusion distance compared to those of conventional catalyst pellets used in fixed-bed reactors. Fibers can be shaped into different geometries suitable for a variety of applications, which makes their installation economically more attractive than monolithic catalysts. Fibers, either woven or knitted, also act as a static mixer, which is not readily feasible with monolithic structures. The staging of fiber layers is arranged by placing them in such a way that channeling is prevented as the elements are alternatingly stacked, providing redistribution of gases. In a recent review paper,[20] the properties of and application of fibers and cloths and their application in multifunctional reactors are discussed thoroughly. The small diameters of the fibers can eliminate the diffusion resistance as the rate-determining step in the overall process.[20] Previously, we have demonstrated the application of fibrous catalysts in gas-phase and liquid-phase reactions.[21−23] The aim of the present study is to apply a knitted silica-fiber support[24] in gas-phase hydrogenation of *o*-xylene. The effect of textural properties of the support and the metal precursor on the catalyst activity and stereoselectivity is studied.

Experimental Section

Support and Catalyst Preparation. A hybrid (organic−inorganic) fiber consisting of cellulose (ca. 67%), poly(silicic acid) (ca. 30%), and sodium aluminate (ca. 3%) was used as the raw material for support preparation. Heat treatment of these fibers up to temperatures of 873−1223 K results in burning of the cellulose component and formation of a coherent filament of silica/silica aluminate (Figure 1a). The X-ray diffraction (XRD) pattern of the silica fiber exhibited an amorphous character.

* To whom correspondence should be addressed. Present address for A. Kalantar Neyestanaki: Nynäs Naphthenics AB, Oljeraffinaderiet, SE-14982 Nynäshamn, Sweden. Fax: +46-8-52020743. E-mail: ahmad.kalantar@nynas.com.

† Åbo Akademi.

‡ University of Turku.

10.1021/ie020827x CCC: $25.00
Published on Web 06/11/2003

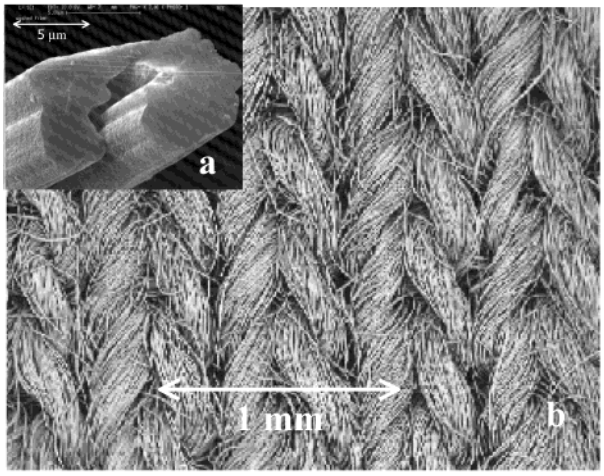

Figure 1. SEM image of a single fiber (a) and the knitted silica-fiber support (b).

Preparation of the knitted silica-fiber support involved knitting of the hybrid fiber yarns and subsequent heat treatment as follows. Yarns from the fibers were double-knitted by laboratory machineries to obtain a textile weighing 530 g/m^2. The obtained textile was treated to remove the impurities from the spinning bath. Heat treatment of the prepared textile at temperatures exceeding 873 K results in the formation of silica fibers retaining their knitted structures (Figure 1b) having a thickness of ca. 1.5 mm. XRD analysis of the catalyst support exhibited an amorphous pattern. The chemical composition of the support measured by a direct current plasma technique (DCP; Spectrasapan IIIA Spectrometrics) was Si = 95.26 wt %, Al = 3.15 wt %, and Na = 1.59 wt % corresponding to the chemical formula (computed by stoichiometry) of $Na_{0.59}Al_1Si_{29.05}O_{59.92}$.

The knitted silica-fiber supports prepared by heat treatment of the hybrid textile at 973, 1073, and 1173 K were used as support materials. Different supported platinum catalysts were prepared by impregnation and adsorption of the support (precalcined at different temperatures) with solutions of hexachloroplatinic acid, platinum nitrate, and platinum tetramine chloride, which are in sequence referred to as Cl, N, and A catalyst; e.g., the (5.0)Pt-SF-1173-A represents a catalyst containing 5 wt % platinum prepared from a platinum tetramine solution, where the support material was heat-treated at 1173 K.

Catalyst Characterization. The Brunauer−Emmett−Teller specific surface area and specific pore volume of the support material were determined by N_2 physisorption using a sorptometer (Sorptomatic 1900, Carlo Erba Instruments). The metal dispersion and mean metal particle diameter were determined by hydrogen adsorption (Sorptomatic 1900). The adsorption isotherms were obtained at 298 K and pressures of 0.13−13.3 kPa. The amount of reversibly adsorbed hydrogen was determined by a backsorption method. Extrapolation of the adsorption isotherms to zero pressure was used to determine the amount of irreversibly adsorbed hydrogen. Prior to the hydrogen adsorption, the catalyst was reduced in situ under hydrogen flow at 673 K for 2 h. Dissociative adsorption of hydrogen was adopted and the metal particle size was determined by assuming spherical particle geometry.

Temperature-programmed desorption (TPD) of ammonia, hydrogen, and *o*-xylene was carried out in a volumetric equipment (AutoChem 2910, Micromeritics) in the temperature range of 298−873 K. Prior to the adsorption studies, the sample was reduced in situ *under hydrogen flow* at 673 K. The sample was then flushed with helium (99.999 vol % purity) at 673 K and cooled under helium flow to 343 K. The *o*-xylene adsorption was carried out by a pulse adsorption technique at 343 K. This was followed by flushing the sample at 373 K with helium for 30 min prior to the TPD measurement. Desorbed gases were identified and analyzed by a quadruple mass spectrometer (Omnistar, Baltzer Instruments). In *o*-xylene-TPD experiments, the mass spectrometer was as well calibrated for the fragmentation compounds. Desorption enthalpies were determined by varying the heating rates from 2.5 to 15 K/min.

Surface and subsurface compositions of the catalyst were investigated with a scanning electron microscope (SEM; Leica Cambridge, Stereoscan 360) equipped with an energy-dispersive X-ray analyzer (EDXA) and X-ray photoelectron spectroscopy (XPS; Perkin-Elmer 5400).

Catalyst Testing. The activity of the fibrous catalysts was studied in a continuous-flow tube reactor with an inner diameter of 10 mm at a gas hourly space velocity (GHSV) of 11 000 h^{-1} and temperatures of 360−460 K in 10 K intervals at atmospheric pressure. The *o*-xylene partial pressure was kept at the constant value of 0.06 bar, whereas the partial pressure of H_2 (AGA, 99.9999 vol %) was varied between 0.36 and 0.73 bar. Argon (AGA, 99.9999 vol %) was used as the makeup gas, keeping a constant GHSV. The experimental conditions corresponded to the hydrogen-to-*o*-xylene molar ratio of 6−12. The gas flows were controlled by means of mass flow controllers (Brooks). The catalyst temperature was measured by use of a K-type thermocouple coaxially inserted into the catalyst bed. *o*-Xylene was pumped by a high-performance liquid chromatography pump (2150 HPLC pump, LKB Bromma) to an evaporator (Bronkhorst) maintained at 443 K and was further driven by argon. All of the lines after the evaporator and the reactor were heated. Products were analyzed by a Varian gas chromatograph (GC) equipped with a 60 m HP-1 column (cross-linked methylsiloxane) and a flame ionization detector. The gas separation was done isothermally (373 K), and the products were further analyzed and confirmed by GC−MS (HP 6890-5973 Instrument). Prior to the activity measurement, the catalyst was reduced in situ under hydrogen flow at 676 K for 2 h. This was followed by cooling of the catalyst under hydrogen flow to the desired temperature, after which the reactant mixture was switched to the reactor.

Results and Discussion

Surface Properties. The results from the N_2-physisorption and H_2-adsorption experiments are listed in Table 1. An increase in the calcination temperature of the hybrid fiber results in a decreased surface area and specific pore volume of the formed knitted silica-fiber support. The changes in the fiber diameters as a function of the calcination temperature were determined by SEM. Totally, 14−33 measurements were carried out for different samples. Gaussian fits of the distribution of the fiber diameters are displayed in Figure 2. As shown, an increase of the calcination temperature from 973 to 1173 K resulted in a decreased fiber diameter from ca. 10.5 to 9 μm. The supports calcined at 1073 and 1173 K exhibited rather similar thread diameters.

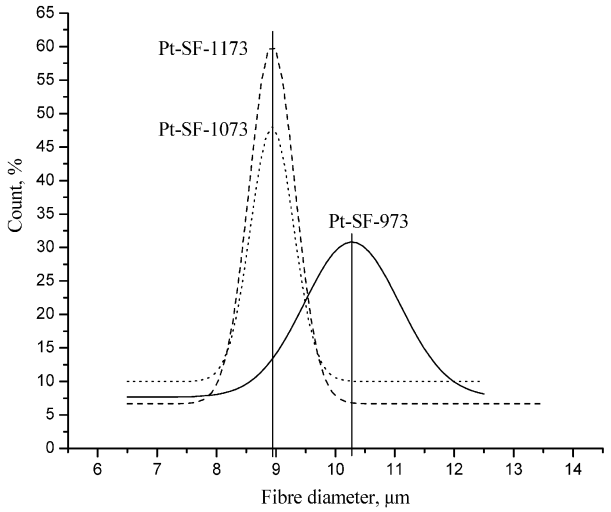

Figure 2. Gaussian fit of the fiber diameter distribution in different supports. Solid line: Pt-SF-973. Dotted line: Pt-SF-1073. Broken line: Pt-SF-1173.

Table 1. Metallic and Textural Properties of the Support and Catalyst

	support		catalyst	
	specific surface, m^2/g	pore volume, cm^3/g	dispersion, %	particle size, nm
(5.0)Pt-SF-1173-Cl	80.9	0.187	32.3	3.2
(5.0)Pt-SF-1073-Cl	137.9	0.313	43.6	2.3
(5.0)Pt-SF-973-Cl	184.4	0.411	52.9	1.9
(2.1)Pt-SF-1173-A	80.9	0.187	69.5	1.5
(3.2)Pt-SF-1073-A	137.9	0.313	69.3	1.5
(4.9)Pt-SF-973-A	184.4	0.411	71.8	1.4
(5.0)Pt-SF-1173-N	80.9	0.187	44.4	2.3

Table 2. Surface Composition of the Fiber-Supported Catalysts (T = 460 K, $p_{o-\text{xylene}}$ = 0.06 bar, GHSV = 11 000 h^{-1})

	Pt-SF-1173-Cl			Pt-SF-1173-A		
	Cl/Pt	Cl/Al	Cl/Na	Cl/Pt	Cl/Al	Cl/Na
freshly dried	3.260	1.287	1.679	0.326	0.13	0.354
reduced at 673 K	0.169	0.059	0.076	0.039	0.01	0.030

Such a fiber shrinkage is in good agreement with N_2-physisorption data (Figure 2 and Table 1).

For the catalysts prepared by the impregnation-to-dryness method from a hexachloroplatinic acid precursor, the metal dispersion values follow the support surface area; the higher the support surface area, the higher the dispersion. The catalysts prepared by adsorption from the tetramine platinum chloride solution, though exhibiting lower uptake for low surface area support, had similar mean platinum particle sizes (Table 1).

The EDXA of the catalysts is presented in Table 2. As expected, the freshly prepared ex chloroplatinic acid catalyst retained the majority of its chlorine, whereas only a small fraction of the initial chlorine is detected on the catalysts prepared by adsorption from a platinum tetramine solution. Catalyst reduction at 673 K resulted in a substantial removal of the surface chlorine; meanwhile, the reduced ex chloroplatonic acid catalyst contained ca. 4 times higher surface chlorine than its corresponding ex platinum tetramine catalyst (Table 2).

The XPS analysis of the reduced samples was carried out to investigate the surface and oxidation states. The Pt 4f binding energies (BEs) were found to be 70.1, 70.3, and 70.6 eV for (5)Pt-SF-1173-N, (5)Pt-SF-1173-Cl, and (2.1)Pt-SF-1173-A, respectively. The XPS data indicate that platinum in the ex nitrate catalyst is in a metallic state after hydrogen treatment at 673 K. A slightly higher BE (70.3 eV) was observed for (5)Pt-SF-1173-Cl catalyst, which might indicate a small charge of the Pt particles; however, such a shift of ca. 0.2 eV in the BE is within the experimental error. On the other hand, the Pt 4f BE of 70.6 eV is an indication of the presence of positively charged platinum particles ($Pt^{+\delta}$) on the ex platinum tetramine catalyst (Pt-SF-1173-A).

Table 3. Behavior of the Knitted Silica-Fiber-Supported Catalysts (T = 460 K, $p_{o-\text{xylene}}$ = 0.06 bar, GHSV = 11 000 h^{-1})

p_{H_2}, bar	(5)Pt-SF-Cl			(4.9)Pt-SF-973-A	(5)Pt-SF-1173-N
	973 K[a]	1073 K	1173 K		
			Conversion, %		
0.36	26.9	20.2	17.0	30.1	78.5
0.49	45.1	32.8	27.9	54.9	85.7
0.61	63.5	51.9	30.9	76.0	98.7
0.73	85.9	73.0		93.5	
			TOF × 10^3, s^{-1}		
0.36	61.8	47.3	56.1	59.4	184.3
0.49	103.6	76.9	92.6	108.3	201.2
0.61	145.9	121.6	102.7	149.9	231.2
0.73	196.5	171.1		184.4	

[a] Support calcination temperature.

***o*-Xylene Hydrogenation.** High conversion levels in *o*-xylene hydrogenation (up to 99%) were obtained over the prepared Pt/knitted silica-fiber catalysts (Table 3). *Cis*-1,2-Dimethyl- and *trans*-1,2-dimethylcyclohexane (1,2-DMCH) were the only reaction products observed. Time-on-stream catalyst deactivation took place, and a steady state was attained after ca. 25 min. The kinetic data presented, hereafter, are obtained under steady-state conditions. The catalyst prepared from the nitrate precursor exhibited a much higher conversion as compared to the corresponding catalysts prepared from chloroplatinic acid and platinum tetramine precursors. An increase of the hydrogen partial pressure resulted in an improved catalyst activity: at H_2/*o*-xylene molar ratios of 12 (p_{H_2} = 0.73 bar), the ex platinum tetramine catalysts (Pt-SF-A) exhibited an activity similar to that of the (5)Pt-SF-1173-N catalyst (Table 3). The performances of the catalysts in terms of the turnover frequency (TOF), calculated from the exposed surface platinum atoms, are summarized in Table 3. The present data indicated the impairing effect of surface chlorine on the hydrogenation activity. The TOF in *o*-xylene hydrogenation over catalysts prepared from the chloroplatinic acid precursor, where a small amount of residual chlorine was present on the surface (Table 2), was much lower than that of the ex nitrate catalyst even for similar platinum particle size catalysts (Pt-SF-1073-Cl vs Pt-SF-1173-N).

The result indicated that for the (5)Pt-SF-Cl catalysts an increased Pt-particle size, induced by an increased calcination temperature of the support (Table 1), results in a decreased catalytic activity (Table 3). This is also reflected in the catalyst activity in terms of TOF (Table 3), where higher TOFs were obtained with the catalyst with smaller platinum particles. An exception was observed for the (5)Pt-SF-1073-Cl, where lower TOFs are observed at lower hydrogen partial pressures (0.36 and 0.49 bar). The structure sensitivity of the xylene hydrogenation has also been reported for palladium, ruthenium, and platinum systems.[8,11,18,19]

Table 4. Product Stereoselectivity at 460 K and $p_{o-\text{xylene}}$ = 0.06 bar (GHSV = 11 000 h^{-1})

	cis-to-trans ratio over						
	(5)Pt-SF-Cl			Pt-SF-A			
p_{H_2}, bar	973 K[a]	1073 K	1173 K	(4.9) 973 K	(3.2) 1073 K	(2.1) 1173 K	(5)Pt-SF-1173-N
0.36	1.11	1.03	1.27	1.23	1.23	1.21	0.7
0.49	1.17	1.15	1.29	1.26	1.24	1.22	0.7
0.61	1.19	1.21	1.16	1.22	1.19	1.22	0.7
0.73	1.2	1.23		1.05	0.88	1.01	

[a] Support calcination temperature.

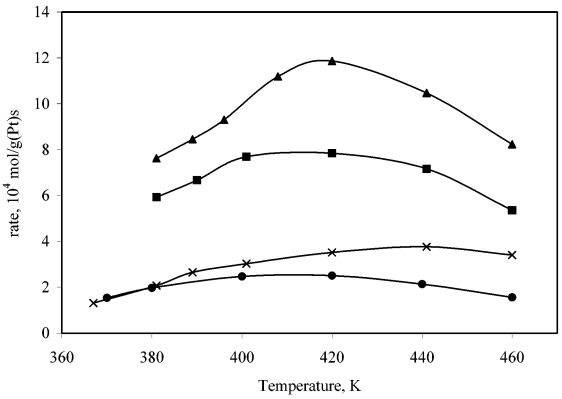

Figure 3. Effect of temperature on the activity of the Pt-SF catalysts. p_{H_2} = 0.36, $p_{o-\text{xylene}}$ = 0.06 bar; (5.0)Pt-SF-973-Cl at p_{H_2} = 0.73 bar: (●) (4.9)Pt-SF-973-A; (■) (3.2)Pt-SF-1073-A; (▲) (2.1)-Pt-SF-1173-A; (×) (5.0)Pt-SF-1173-Cl.

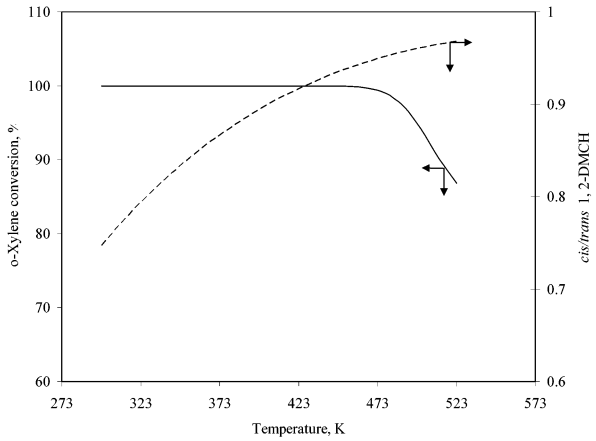

Figure 4. Thermodynamic equilibrium in *o*-xylene hydrogenation, $p_{o-\text{xylene}}$ = 0.06 and p_{H_2} = 0.36 bar. Solid line: *o*-xylene conversion. Broken line: cis-to-trans 1,2-DMCH ratio.

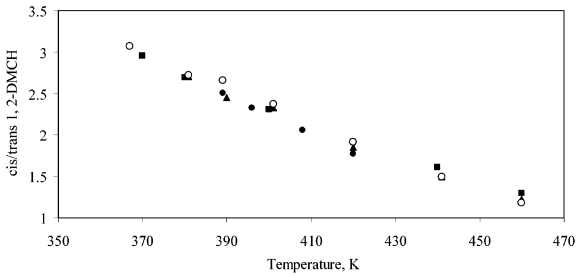

Figure 5. Temperature dependency of the cis-to-trans 1,2-DMCH ratio. p_{H_2} = 0.37, $p_{o-\text{xylene}}$ = 0.06 bar: (■) (4.9)Pt-SF-973-A; (▲) (3.2)Pt-SF-1073-A; (●) (2.1)Pt-SF-1173-A; (○) (5.0)Pt-SF-1173-Cl.

A reversible maximum in the catalyst activity vs temperature was observed for all of the catalysts (Figure 3). A similar temperature dependency of the catalyst activity in *o*-xylene hydrogenation has also been reported over Ni and Pt catalysts.[12−15,17] Although the catalysts prepared from platinum tetramine exhibited similar metallic dispersions, and therefore similar mean platinum particle sizes (Table 1), they performed differently in *o*-xylene hydrogenation (Tables 3 and 4 and Figure 3). The result indicated a higher activity with the catalyst having the lowest surface area and platinum loading, i.e., (2.1)Pt-SF-1173-A (Figure 3). This observation might be a result of diffusion limitation over the catalysts as a result of their different morphologies. As mentioned before, the N_2-physisorption experiments indicated a decreased pore volume (Table 1) and closure of small-diameter pores by increased support calcination temperature. The fiber shrinkage takes place by an increased support calcination (preparation) temperature. A decrease of the fiber diameter will result in a decreased diffusion length and, consequently, diffusion limitations are suppressed (note that the catalyst was operated at high conversion levels).

Stereoselectivity. Thermodynamic equilibrium calculations of the gas composition and temperatures used indicated that *trans*-1,2-DMCH is the thermodynamically favored product (Figure 4). However, as is demonstrated in Table 4 and Figure 5, the stereoselectivity is strongly affected by the operation conditions and the active metal precursor. The catalyst prepared from a platinum nitrate precursor exhibited a higher selectivity to the formation of the trans isomer, whereas the cis isomer was formed in a higher rate over ex chloroplatinic acid and ex platinum tetramine catalysts (Table 4). The observed differences in the ratios of cis and trans isomers are not fully the consequence of the product stereoselectivity dependency on conversion levels: the catalysts prepared from Cl-containing precursors, at similar conversion levels (though different hydrogen partial pressures), exhibited a higher selectivity to the formation of the cis isomer (Tables 3 and 4 and Figure 6) as compared to the ex nitrate catalyst. The observed stereoselectivities cannot be directly attributed to the particle size differences because the ex-nitrate catalyst and Pt-SF-1073-Cl catalyst having similar particle sizes still exhibited different stereoselectivities.

The selectivity toward the formation of the thermodynamically favored trans isomer over the catalysts prepared from chloroplatinic acid (Pt-SF-Cl catalysts) is increased by a decreased mean platinum particle diameter (Tables 1 and 4). An increase in the hydrogen partial pressure decreased the selectivity to trans-isomer formation, with the exception of the (5)Pt-SF-1173-Cl catalyst, where a slightly increased selectivity toward the trans-isomer formation was observed. The catalysts prepared from platinum tetramine precursor (Pt-SF-A catalysts) had similar platinum particle sizes (ca. 1.4 nm) and also exhibited similar stereoselectivities. Here, in contrast to the Pt-SF-Cl catalysts, increased hydrogen partial pressures up to 0.61 bar did not have any significant effect on the cis-to-trans ratios (Table 4). At higher hydrogen partial pressures, the

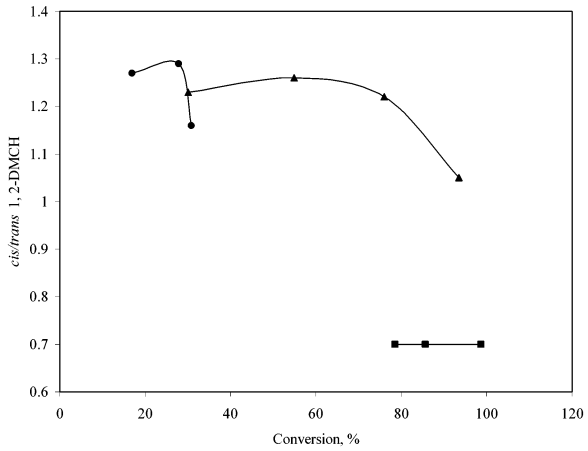

Figure 6. Product distribution (cis-to-trans ratio) dependency on the conversion levels, $p_{o-\text{xylene}} = 0.06$ bar: (▲) (4.9)Pt-SF-973-A; (●) (5.0)Pt-SF-1173-Cl; (■) (5.0)Pt-SF-1173-N.

Scheme 1. *o*-Xylene Hydrogenation and Stereoselectivity According to the Rollover Mechanism

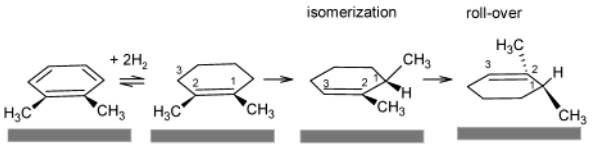

selectivity to the trans-isomer formation was sharply enhanced. The cis-to-trans ratio over all of the catalysts was found to decrease by increased operation temperature (Figure 5). Such a temperature dependency of the stereoselectivity has been reported previously for xylene hydrogenation over Pd, Ru, Ni, and Pt catalysts.[8,11,12−15,18]

o-Xylene is believed to adsorb on noble metal surfaces with the aromatic ring parallel to the surface.[25,26] To relieve the steric repulsion, the two CH_3 groups should direct away from the surface. In this way, the hydrogenation of the aromatic ring results in the formation of a cis isomer, i.e., the kinetically favored product. The formation of a trans isomer has been explained by a rollover mechanism[8−14,16−19] proposed originally by Inoue et al.[27] (Scheme 1). The mechanism explains the formation of *trans*-1,2-DMCH as the last double bond to be hydrogenated isomerizes; i.e., 1,2-dimethylcyclohexene isomerizes to 2,3-dimethylcyclohexene. The rollover of the latter one provides the necessary condition for the formation of *trans*-1,2-DMCH.

TPD Studies. As pointed out, the rate of *o*-xylene hydrogenation vs temperature passes through a maximum (Figure 3) that is not associated with the thermodynamic equilibrium (Figure 4). Such a temperature dependency of the hydrogenation rate could principally be the consequence of decreased surface coverage of the reactants. To investigate the surface coverage of reactants, H_2- and *o*-xylene-TPD experiments were carried out. The H_2-TPD data indicated the presence of surface hydrogen in the temperature range studied. The amount of H_2 desorbed in the temperature range of 303−873 K was measured and were 0.012, 0.05, and 0.11 mmol/$g_{catalyst}$ for (5.0)Pt-SF-1173-N, (5.0)Pt-SF-1173-Cl, and (4.9)Pt-SF-973-A, respectively. The relatively higher hydrogen desorption from the ex platinum tetramine catalyst is due to its higher metallic dispersion. The other reason for the higher hydrogen uptake of the catalyst prepared from Cl-containing salts might be due

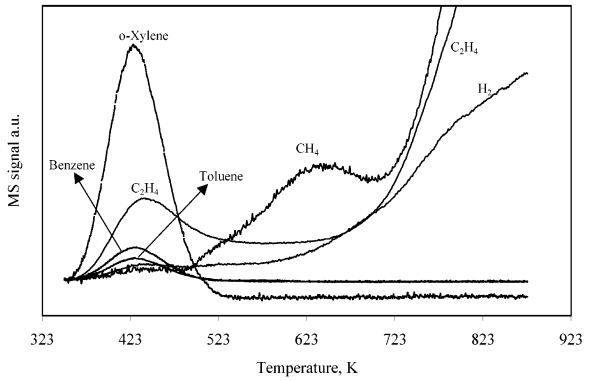

Figure 7. *o*-Xylene-TPD pattern of the (4.9)Pt-SF-973-A catalyst. Heating rate: 10 K/min.

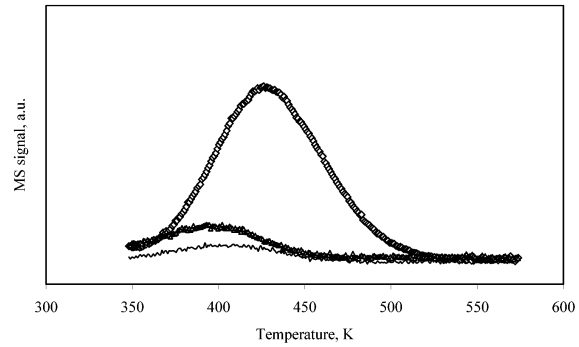

Figure 8. *o*-Xylene-TPD patterns of different supported−supported catalysts: (△) (5.0)Pt-SF-1173-Cl; (◇) (4.9)Pt-SF-973-A; (—) (5.0)Pt-SF-1173-N.

to the effect of the surface residual chlorine anions on the hydrogen uptake.

The *o*-xylene-TPD patterns of the fibrous catalysts are given in Figures 7 and 8. Single *o*-xylene desorption patterns were observed along the hydrogenolysis products, toluene and benzene, following the same desorption pattern as that of *o*-xylene. Ethene, methane, and hydrogen were also detected, the rate of desorption of which sharply increased at temperatures exceeding 573 K. The peak maxima in the *o*-xylene desorption over (5.0)Pt-SF-1173-Cl and (5.0)Pt-SF-1173-N were close and peaked at ca. 403 K. On the other hand, the maximum in the *o*-xylene desorption from the (4.9)Pt-SF-973-A is shifted to higher temperature (ca. 433 K), which coincides with the temperature of maximum activity in *o*-xylene hydrogenation (Figure 3). The *o*-xylene-TPD results indicate a decreased *o*-xylene surface coverage at temperatures exceeding 430 K, which ultimately results in a decreased hydrogenation rate. The Pt-SF1173-A (with an average platinum diameter of 1.46 nm) catalyst exhibited a broadened *o*-xylene desorption pattern (Figure 8) as compared to the ex nitrate and ex chloroplatinic acid catalysts, having larger platinum particles (Table 1). Such broadenings are thought to be the consequence of nonuniformity of the surface platinum sites, with different adsorption affinities. The properties of small metal particles are influenced by the support resulting in the formation of sites with different adsorption capacities (amounts). In such cases, the thermal desorption pattern is a sum of desorbed molecules from sites with different adsorption capacities.[28] The *o*-xylene desorption enthalpies from the Pt-SF-1173-Cl and Pt-SF-1173-A catalysts were determined and found to be 46 and 39 kJ/mol, respectively. The relatively lower ad-

sorption enthalpy of *o*-xylene desorption from the ex platinum tetramine catalyst, as compared to the ex chloroplatinic acid catalyst, is also believed to be due to the adsorption centers as mentioned.

Aromatics are believed to adsorb flat on the group VIII metals surface via π bonding, which involves an electron transfer from the aromatic ring to the unoccupied d-metal orbitals followed by a backdonation of an electron from the metal to the π*-antibonding orbital of aromatics. The aromatic ring adsorption also depends on the local electron density of the metal atom. Catalysts with small particle sizes of the active metallic component exhibit a decreased d-shell occupation and density of states at the Fermi level.[29] This decreased electron occupation in the valence bond leads to an increased BE of species behaving as Lewis bases such as *o*-xylene. An additional electron withdrawal induced by the presence of chlorine anions in the support−platinum interface will result in a further decrease of the d-shell occupation and hence increases in the BEs of the adsorbed species involved. Such increased *o*-xylene adsorption can be seen from the *o*-xylene-TPD patterns (Figure 8), where the Pt-SF-N catalyst, while being the most active catalyst, exhibited a much lower *o*-xylene adsorption. The Pt-SF-A catalyst had the highest *o*-xylene desorption, which is believed to be due to the electron-deficient nature of the platinum particle as a result of the combined effect of the residual chlorine and smaller platinum particle sizes (Tables 1 and 2).

To verify the electron-deficient nature of the Pt particles, NH_3-TPD experiments were carried out in the temperature range of 303−873 K. Indeed, the catalyst prepared from the platinum tetramine salt desorbed an order of magnitude more ammonia than the other two catalysts. The amounts of ammonia desorbed from the catalyst were 0.06, 0.04, and 0.53 mmol/$g_{catalyst}$ for (5.0)-Pt-SF-1173-N, (5.0)Pt-SF-1173-Cl, and (4.9)Pt-SF-973-A, respectively. As mentioned previously, the XPS data also indicated the presence of positively charged Pt particles on the ex platinum tetramine catalyst.

An increased adsorption strength might have a negative impact on the aromatic ring hydrogenation rate. Moreover, less electron transfer from $Pt^{+\delta}$ to the π*-antibonding orbital of the aromatic ring of the chemisorbed xylene can cause the activity of the aromatic ring to decrease, consequently decreasing the hydrogenation rate (Pt-SF-Cl catalysts). Such a deteriorating effect of chlorine has been reported on hydrogenation of phenol and styrene, where lower hydrogenation rates have been observed over the palladium catalysts prepared from chloride salts.[30,31] In the present study, the reason for the lower activity of the catalyst prepared from chloroplatinic acid, and to a much lesser extent for ex platinum tetramine catalysts, is due to this negative impact of residual surface chlorine on the hydrogenation rate. In the same manner, the residual chlorine affects the stereoselectivities by lowering the rate of rollover of 1,2-dimethylcyclohexene (Scheme 1).

Conclusions

The result of the present study indicated the suitability of the prepared Pt/knitted silica fibers in gas-phase hydrogenation of *o*-xylene because high conversion levels of *o*-xylene were achieved. Differences in the textural properties of the support material, as well as the Pt precursor, affect the performance of the catalyst. Residual surface chlorine declined the catalyst activity and influenced the product stereoselectivity because the catalyst prepared from Cl-containing Pt precursors favored the formation of the cis isomer. Higher hydrogenation rates along with an increased selectivity of the thermodynamically favored *trans*-1, 2-DMCH were attained over the catalyst prepared from the platinum−nitrate precursor. The selectivity of the cis isomer was decreased linearly by increasing the operation temperature. A temperature dependency of the hydrogenation rate with a profound optimal temperature was observed. The TPD experiments indicated that the decreased surface coverage of *o*-xylene with the temperature increase might be the reason for the observed temperature behavior of the hydrogenation rate.

Acknowledgment

The financial support from the Academy of Finland is gratefully acknowledged. This work is a part of the activities at the Åbo Akademi Process Chemistry Group within the Finnish Center of Excellence Program (2000-2005) by the Academy of Finland.

Literature Cited

(1) Smeds, S.; Murzin, D.; Salmi, T. Kinetics of Ethylbenzene Hydrogenation on Ni/Al_2O_3. *Appl. Catal.* **1995**, *125*, 271.

(2) Smeds, S.; Salmi, T.; Murzin, D. Kinetics of Mesitylene Hydrogenation on Ni/Al_2O_3. *Appl. Catal. A* **1999**, *185*, 131.

(3) Smeds, S.; Salmi, T.; Murzin, D. Gas-phase hydrogenation of ethylbenzene over Ni.; Comparison of different laboratory fixed bed reactors. *Appl. Catal. A* **2000**, *201*, 55.

(4) Lin, S. D.; Vannice, M. A. Hydrogenation of Aromatic Hydrocarbons over Supported Pt Catalysts. I. Benzene Hydrogenation. *J. Catal.* **1993**, *143*, 539.

(5) Lin, S. D.; Vannice, M. A. Hydrogenation of Aromatic Hydrocarbons over Supported Pt Catalysts. II. Toluene Hydrogenation. *J. Catal.* **1993**, *143*, 554.

(6) Lin, S. D.; Vannice, M. A. Hydrogenation of Aromatic Hydrocarbons over Supported Pt Catalysts. III. Reaction Models for Metal Surfaces and Acidic Sites on Oxide Supports. *J. Catal.* **1993**, *143*, 563.

(7) Rahaman, M. V.; Vannice, M. A. The Hydrogenation of Toluene and *o*-, *m*- and *p*-Xylene over palladium. I. Kinetic Behavior and *o*-Xylene Isomerization. *J. Catal.* **1991**, *127*, 251.

(8) Viniegra, M.; Córdoba, G.; Gómez, R. Gas-phase Hydrogenation of *o*-Xylene over Palladium Catalysts. *J. Mol. Catal.* **1990**, *58*, 107.

(9) Martin, N.; Córdoba, G.; López-Gaona, A.; Viniegra, M. Gas-Phase Hydrogenation of *m*-Xylene on Palladium. *React. Kinet. Catal. Lett.* **1991**, *44*, 381.

(10) Cordoba, G.; Fierro, J. L. G.; López-Goana, A.; Martin, N.; Viniegra, M. Probing $Ru-Pd/SiO_2$ Catalysts by Gas-Phase *o*-Xylene Hydrogenation. *J. Mol. Catal., A: Chem.* **1995**, *96*, 155.

(11) Viniegra, M.; Martin, N.; López-Gaona, A.; Córdoba, G. Gas-Phase Hydrogenation of *o*-Xylene on Ru Supported Catalysts. *React. Kinet. Catal. Lett.* **1993**, *49*, 353.

(12) Smeds, S.; Salmi, T.; Murzin, D. Gas-phase hydrogenation of *o*- and *p*-xylene on Ni/Al_2O_3—Kinetic behaviour. *Appl. Catal. A* **1996**, *145*, 253.

(13) Smeds, S.; Murzin, D.; Salmi, T. Kinetics of *m*-Xylene Hydrogenation on Ni/Al_2O_3. *Appl. Catal. A* **1996**, *141*, 207.

(14) Smeds, S.; Salmi, T.; Murzin, D. Gas-Phase Hydrogenation of *o*- and *p*-Xylene on Ni/Al_2O_3—Kinetic Modeling. *Appl. Catal. A* **1997**, *150*, 115.

(15) Keane, M. A. The Hydrogenation of *o*-, *m*-, and *p*-Xylene over Ni/SiO_2. *J. Catal.* **1997**, *166*, 347.

(16) Aramendía, M. A.; Borau, V.; Jiménez, C.; Marinas, J. M.; Rodero, F.; Sempre, M. E. Hydrogenation of Xylenes over Supported Pt catalysts. Influence of Different Variables on their Catalytic Activity. *React. Kinet. Catal. Lett.* **1992**, *46*, 305.

(17) Saymeh, R. A.; Asfour, H. M. Kinetic Study of the Gas-Phase Hydrogenation of *o*-Xylene over Pt/Al_2O_3 Catalyst. *Orient. J. Chem*. **2000**, *16*, 67.

(18) Saymeh, R. A.; Asfour, H. M.; Tuaimen, W. A. Gas Phase Study of *o*-Xylene Hydrogenation over Pt/Al_2O_3: The Influence of Ce and the Catalyst Reduction Temperature on selectivity. *Asian J. Chem*. **1997**, *9*, 350.

(19) Saymeh, R. A.; Asfour, H. M.; Tuaimen, W. A. Gas Phase Study of *o*-Xylene Hydrogenation over Pt/Al_2O_3: Influence of the Catalyst Reduction Temperature. *Ind. J. Chem*. **1997**, *36B*, 799.

(20) Matov-Meytal, Yu.; Sheintuch, M. Catalytic Fibers and Cloths. *Appl. Catal. A* **2002**, *231*, 1.

(21) Kalantar Neyestanaki, A.; Lindfors, L.-E. Catalytic Combustion of Propane and Natural Gas over Silica-Fibre Supported Catalysts. *Combust. Sci. Technol*. **1994**, *97*, 121.

(22) Salmi, T.; Mäki-Arvela, P.; Toukoniitty, E.; Kalantar Neyestanaki, A.; Tiainen, L.-P.; Lindfors, L.-E.; Sjöholm, R.; Laine, E. Liquid-Phase Hydrogenation of Citral over an Immobile Silica Fibre Catalyst. *Appl. Catal. A* **2000**, *196*, 93.

(23) Toukoniitty, E.; Mäki-Arvela, P.; Kalantar Neyestanaki, A.; Salmi, T.; Sjöholm, R.; Leino, R.; Laine, E.; Kooyman, P.; Ollonqvist, T.; Väyrynen, J. Batchwise and Continuous Enantioselective Hydrogenation of 1-Phenyl-1,2-propanedione Catalyzed by New Pt/SiO_2 Fibers. *Appl. Catal. A* **2001**, *216*, 73.

(24) Salanne, S.; Kalantar Neyestanaki, A.; Lindfors, L.-E.; Vapaaoksa, P. Finnish Patent 89012, 1993.

(25) Peck, J. W.; Koel, B. E. Selective Dehydrogenation of 1,3-Cyclohexadiene on Ordered Sn/Pt(111) Surface Alloys. *J. Am. Chem. Soc*. **1996**, *118*, 2708.

(26) Koel, B. E.; Blank, D. A.; Carter, E. A. Thermochemistry of the Selective Dehydrogenation of Cyclohexane to Benzene on Pt Surfaces. *J. Mol. Catal. A: Chem*. **1998**, *131*, 39.

(27) Inoue, Y.; Herrmann, J. M.; Schmidt, H.; Burwell, R. L.; Butt, J. B.; Cohen, J. B. Pt/SiO_2. IV. Isotopic Exchange between Cyclopentane and Deuterium. *J. Catal*. **1978**, *53*, 401.

(28) Tovbin, Yu. K.; Votaykov, E. V. Analysis of Thermal Desorption Spectra of Heterogeneous Surfaces. *Langmuir* **1999**, *15*, 6070.

(29) Baetzold, R. C. Size and Geometric effects in Copper and Palladium Metal Clusters. *J. Phys. Chem*. **1978**, *82*, 738.

(30) Sepuldeva, J.; Figoli, N. Effect of Residual Chlorine on the Activity of Pd/SiO_2 Catalysts during the Selective Hydrogenation of Styrene. *React. Kinet. Catal. Lett*. **1994**, *53*, 155.

(31) Mahata, N.; Vishwanathan, V. Influence of Palladium Precursors on Structural Properties and Phenol Hydrogenation Characteristics of Supported Palladium Catalysts. *J. Catal*. **2000**, *196*, 262.

Received for review October 21, 2002
Revised manuscript received April 28, 2003
Accepted May 6, 2003

IE020827X